ELSEVIER

International Journal of Mass Spectrometry 201 (2000) 321–336

International Journal of Mass Spectrometry

Radical cations of DNA bases: some insights on structure and fragmentation patterns by density functional methods

Roberto Improta, Giovanni Scalmani, Vincenzo Barone*

Dipartimento di Chimica, Università Federico II Via Mezzocannone 4, I-80134 Napoli, Italy

Received 25 November 1999; accepted 15 February 2000

Abstract

In this work the DNA bases and their radical cations are investigated by an hybrid Hartree-Fock/density functional model. The calculated geometries and ionization energies are in good agreement with the available experimental data, confirming the reliability of this approach for the study of open shell systems. A critical comparison between the electronic and geometric structures of the radical cations and those of the neutral DNA bases, together with an analysis based on the natural bond orbital theory, offer some insights on the fragmentation patterns recorded in the experimental mass spectra as well as a tentative explanation of the different behavior of thymine and cytosine. (Int J Mass Spectrom 201 (2000) 321–336) © 2000 Elsevier Science B.V.

Keywords: Ab initio calculations; Density functional theory

1. Introduction

The fully theoretical explanation of fragmentation patterns in mass spectra is not an easy task even in the case of small molecules [1,2]: a reaction in which many bonds can be broken and formed is a very complex, and often inherently dynamic, process [3,4]. In principle, it would be necessary to consider all the possible competing reaction paths, studying in-depth all the transition states and the surface crossings. Not only the knowledge of the electronic ground state, but also of the excited states would be required together with the evaluation (up to high energy) of the density of states including all the internal degrees of freedom of the molecule [3]. Moreover in labile high-energy structures, the electronic states can be strongly geometry-sensitive, leading to the breakdown of the Born-Oppenheimer approximation [5,6].

Notwithstanding all this, the value of an useful interaction between experimentalists and theoreticians in the advance of mass spectroscopy has already been assessed [7].

The application of quantum mechanical (QM) approaches in this field can be more clearly illustrated by considering the different aspects involved in the interpretation of mass spectra [2]. The following points are usually considered: (1) the relative strength of the bonds in the excited state ions, (2) the relative stability of the likely fragment species, (3) the relative probability of entering a decomposition path, and (4) the possibility of rearrangements involving concerted cleavages of bonds and their mechanism.

It is clear that accurate calculations can be of big

* Corresponding author. E-mail: enzo@chemna.dichi.unina.it

PII S1387-3806(00)00225-6

help in dealing with each of these aspects, with a continuously improving effectiveness, as demonstrated by the increasing number of computational papers appeared in the last years on journals devoted to mass spectroscopy [8].

The fast development of computing technologies has indeed enabled researchers to routinely undertake the quantum mechanical study of ground state structures and properties of medium size molecules and ions, with results often approaching the so-called chemical accuracy [9]. This allows for, example, a reliable determination of the relative stability of the several different isomers which can be formed during the fragmentation process. From this point of view the development of computational methods capable of going beyond the Hartree-Fock (HF) model has been of overwhelming importance. In fact, calculations able to properly account for the electron correlation effects (conventional many-body approaches [10] or models based on the density functional theory [11]) are necessary in order to get a reliable description of open shell molecular systems in highly excited (ionized) states, eventually close to dissociation. Moreover, when several electronic states are involved, a study of the reaction mechanism requires the comparison of several potential energy surfaces, which should be determined with the *same* accuracy: HF wave functions often do not meet this requirement.

In addition, the implementation of new effective algorithms has made much easier the location of the saddle points connecting the energy minima, the accurate determination of the energy barriers, as well as the study of the interaction of two crossing electronic surfaces, i.e. the determination of the conical intersections and the evaluation of the non adiabatic couplings among them [12].

All the theoretical procedures for the "chemical interpretation" of the computational results are well assessed: for example, the different methods for assigning atomic charges or bond orders have been thoroughly investigated, determining their physical basis and their possible applications. Finally, the vibrational characterization of species in the ground and in the excited states has also witnessed an impressive development and this is very important since highly reactive species are not easily accessible in experiments.

The potentialities of these recent developments are not restricted to a small group of theoreticians, since the increased availability of user-friendly quantum chemical packages has made quite accurate ab initio calculations accessible also to nonspecialists [13]. At the same time, the theoretical tools (charges, bond orders, etc.) that might be useful for the interpretation of mass spectra are nowadays available in many QM packages.

In this article we will focus our attention almost exclusively on the first of the previous points: the analysis of the electronic and geometric structure of the molecular cations. Using some of the above-cited theoretical tools we will try to determine some "propensity rules" which could explain the fragmentation patterns of the four DNA bases [14,15]. We will indeed analyze the ground state geometric structures and electronic properties of the molecular ions of adenine, cytosine, guanine and thymine (see Fig. 1). The comparison with the neutral parent compounds will also be presented, in order to obtain hints for a qualitative prediction of the most important fragmentation patterns and a rationalization of the main features of the experimental mass spectra. To that purpose, we have also analyzed some features of the fragmentation path of thymine.

It is important to note that the study of the radical cations of DNA bases is in itself interesting: these species are one of the results of the radiation damage to DNA, a process which has attracted significant attention in the last years [16]. Though a large amount of experimental studies have been dedicated to this subject, the reaction mechanism has not yet been firmly assessed and, to some extent, it is also uncertain in which form the radicals are created (cationic, anionic, or neutral form). Moreover, only few reliable theoretical studies on these radicals are available in literature [16,17]: an accurate ab initio study can thus contribute to a better knowledge of these compounds, even if for the in vivo study of the DNA radicals it is important to take into account solvent effects [16].

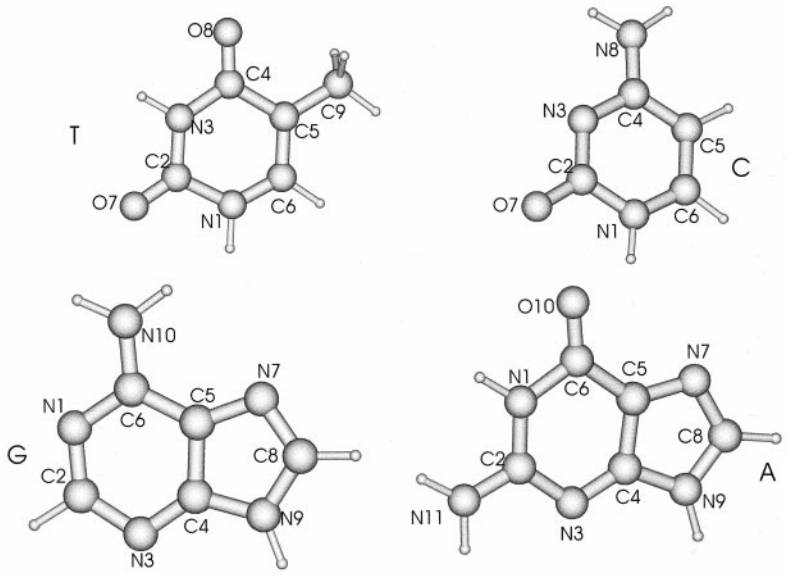

Fig. 1. Atom numbering and optimized geometries of the radical cations of DNA bases: thymine (T), cytosine (C), guanine (G), and adenine (A).

2. Computational details

The molecular ions are open-shell systems and thus properly described by means of unrestricted wave functions which allow each α molecular orbital to be different from the corresponding β one, thus taking into account some amount of electron correlation through spin polarization. Unrestricted calculations have been carried out according to the Kohn-Sham (KS) self-consistent field (SCF) formalism [11]. The gradient corrected hybrid B1LYP functional [18] has been used throughout, together with the gaussian 6-311G(d,p) basis set [19].

Several studies have convincingly shown that methods rooted in the density functional theory (DFT) are well suited to the study of open-shell systems, not only for geometry optimization but also for the evaluation of magnetic properties [20]. In fact, even if DFT does not use, in principle, any well-defined wave function, the expectation value of the S^2 operator can nonetheless be evaluated using a reference set of KS orbitals. This has shown that the problem of spin contamination is usually much less severe in the unrestricted KS model than in the corresponding UHF approach [20].

The geometry of the DNA bases (adenine, cytosine, guanine, and thymine) and of the corresponding radical cations have been fully optimized. This gives access, inter alia, to adiabatic ionization energies (IEs). In addition, single point calculations of the ionic species using the geometry of the neutral ones have been carried out to study the effect of the "vertical ionization process" on the electronic structure.

All the QM calculations have been performed by means of the GAUSSIAN98 package [21].

The electron density of the charged and neutral species has been analyzed according to different schemes in order to evaluate atomic charges and bond orders. In particular, beside the basic Mulliken population analysis (MPA) [22], we have used more sophisticated approaches like the generalized atomic polar tensor (GAPT) atomic charges [23], the natural population analysis (NPA) [24b] and the natural resonance theory (NRT) [24c]. The two latter methods are both based on the natural bond orbital (NBO) theory of Weinhold and co-worker [24a]. These analyses have been performed with an in-house modified version of GAUSSIAN98 capable to compute the GAPT charges and fully interfaced to the NBO 4.0 package [25].

Table 1
Structural parameters of neutral and radical cationic forms of thymine optimized at the B1LYP/6-311G(*d*,*p*) level of theory

Bond length	Expt.[a]	Neutral	Cationic	Bond angle	Expt.[a]	Neutral	Cationic
*N*1–*C*2	1.35	1.388	1.451	*N*1–*C*2–*N*3	115	112.4	112.5
*C*2–*N*3	1.36	1.385	1.371	*C*2–*N*3–*C*4	126	128.2	127.3
*N*3–*C*4	1.39	1.406	1.401	*N*3–*C*4–*C*5	116	114.5	115.7
*C*4–*C*5	1.45	1.469	1.494	*C*4–*C*6–*C*6	118	118.1	119.6
*C*5–*C*6	1.35	1.347	1.407	*C*5–*C*6–*N*1	122	122.8	119.3
*C*6–*N*1	1.38	1.379	1.322	*C*6–*N*1–*C*2	123	123.9	127.4
*C*2–*O*7	1.23	1.209	1.190	*N*1–*C*2–*O*7	123	123.3	118.9
*C*4–*O*8	1.23	1.213	1.201	*N*3–*C*2–*O*7	122	124.2	127.1
*C*5–*C*9	1.50	1.500	1.472	*N*3–*C*4–*O*8	118	120.5	122.0
*N*1–*H*10		1.007	1.018	*C*5–*C*4–*O*8	126	125.0	122.0
*N*3–*H*11		1.011	1.016	*C*4–*C*5–*C*9	119	117.8	118.0
*C*6–*H*12		1.082	1.084	*C*6–*C*5–*C*9	123	124.1	122.5
*C*9–*H*13		1.092	1.098	*C*5–*C*9–*H*13		110.8	109.8
*C*9–*H*14		1.092	1.098	*C*5–*C*9–*H*14		110.8	109.8
*C*9–*H*15		1.091	1.088	*C*5–*C*9–*H*15		111.2	112.9

[a] Reference compound: thymine monohydrate [26].

3. Results and discussion

3.1. Analysis of the neutral DNA bases

In Tables 1–4 are reported the main geometrical parameters for the neutral and radical cationic form of the DNA bases, together with the available experimental data for the neutral compounds. The calculated geometries are in good agreement with the experimental ones: the differences in the bond lengths hardly exceed 0.01 Å and those in the bond angles 1°, thus being close to the limit of the experimental error for the x-ray reference structures [26–29]. The only remarkable exceptions to the above considerations concern the geometries around the carbonyl group. The value of the CO bond distance is slightly underestimated by the B1LYP computations and, correspondingly, the lengths of the other bonds involving the carbonyl carbon atom are slightly overestimated. Thus, B1LYP calculations seem to underestimate the relative weight of the resonance structure involving a single C–O^- bond. However, in the crystal the carbonyl moiety can be engaged in hydrogen bonds (increasing the CO bond length), and this effect could

Table 2
Structural parameters of neutral and radical cationic forms of cytosine optimized at the B1LYP/6-311G(*d*,*p*) level of theory

Bond length	Expt.[a]	Neutral	Cationic	Bond angle	Expt.[a]	Neutral	Cationic
*N*1–*C*2	1.37	1.429	1.415	*N*1–*C*2–*N*3	118	115.9	119.1
*C*2–*N*3	1.36	1.371	1.344	*C*2–*N*3–*C*4	120	120.5	121.0
*N*3–*C*4	1.34	1.314	1.348	*N*3–*C*4–*C*5	122	124.1	120.5
*C*4–*C*5	1.42	1.441	1.432	*C*4–*C*5–*C*6	117	116.0	119.0
*C*5–*C*6	1.34	1.355	1.383	*C*5–*C*6–*N*1	120	120.0	119.1
*C*6–*N*1	1.36	1.353	1.333	*C*6–*N*1–*C*2	123	123.4	121.1
*C*2–*O*7	1.23	1.211	1.236	*N*1–*C*2–*O*7	120	118.3	117.4
*C*4–*N*8	1.33	1.360	1.328	*N*3–*C*2–*O*7	122	125.8	124.2
*N*1–*H*9		1.008	1.016	*N*3–*C*4–*N*8	118	117.1	116.3
*C*5–*H*10		1.079	1.081	*C*5–*C*4–*N*8	120	118.8	121.5
*C*6–*H*11		1.082	1.082	*H*12–*N*8–*H*13		118.5	118.7
*N*8–*H*12		1.007	1.010	*N*3–*C*4–*N*8–*H*12		9.0	0.0
*N*8–*H*13		1.004	1.007	*C*5–*C*4–*N*8–*H*13		−15.2	0.0

[a] See [27].

Table 3
Structural parameters of neutral and radical cationic forms of adenine optimized at the B1LYP/6-311G(*d*,*p*) level of theory

Bond length	Expt.[a]	Neutral	Cationic	Bond angle	Expt.[a]	Neutral	Cationic
*N*1–*C*2	1.35	1.341	1.312	*N*1–*C*2–*N*3	127	128.8	129.8
*C*2–*N*3	1.32	1.333	1.381	*C*2–*N*3–*C*4	112	111.3	112.0
*N*3–*C*4	1.34	1.336	1.298	*N*3–*C*4–*C*5	127	126.8	127.5
*C*4–*C*5	1.36	1.395	1.430	*C*4–*C*5–*C*6	117	116.0	115.6
*C*5–*C*6	1.39	1.409	1.435	*C*5–*C*6–*N*1	117	118.7	119.1
*C*6–*N*1	1.35	1.341	1.355	*C*6–*N*1–*C*2	120	118.4	118.2
*C*4–*N*9	1.36	1.376	1.386	*N*3–*C*4–*N*9	129	128.7	130.4
*C*5–*N*7	1.38	1.384	1.336	*C*5–*C*4–*N*9	105	104.5	103.6
*N*7–*C*8	1.31	1.306	1.343	*C*4–*C*5–*N*7	111	111.4	111.1
*C*8–*N*9	1.35	1.379	1.352	*C*6–*C*5–*N*7	132	132.7	131.1
*C*6–*N*10	1.35	1.350	1.320	*C*5–*N*7–*C*8	104	104.1	104.6
*C*2–*H*11		1.085	1.083	*N*7–*C*8–*N*9	112	113.3	113.1
*C*8–*H*12		1.079	1.080	*C*8–*N*9–*C*4	108	106.8	107.0
*N*9–*H*13		1.007	1.012	*N*1–*C*6–*N*10	117	119.0	118.2
*N*10–*N*14		1.004	1.014	*C*5–*C*6–*N*10	126	122.3	121.5
*N*10–*H*15		1.004	1.012	*H*14–*N*10–*H*15		120.7	120.0

[a] Reference compound: 9-methyl adenine [28].

be even more important in hydrated crystals; as a matter of fact, in the crystal of guanine monohydrate the carbonyl oxygen is hydrogen bonded with the water molecule [29]. This effect can probably explain at least part of the observed discrepancy between experimental and calculated geometries.

Interestingly, the amino groups in cytosine, guanine and adenine are not planar, confirming the final result of a rather debated subject [30].

Table 5 collects the calculated and experimental values of vertical and adiabatic IEs for the four DNA bases. The IEs computed at the B1LYP/6-

Table 4
Structural parameters of neutral and radical cationic forms of guanine optimized at the B1LYP/6-311G(*d*,*p*) level of theory

Bond length	Expt.[a]	Neutral	Cationic	Bond angle	Expt.[a]	Neutral	Cationic
*N*1–*C*2	1.371	1.369	1.356	*N*1–*C*2–*N*3	124.6	123.5	124.7
*C*2–*N*3	1.315	1.307	1.358	*C*2–*N*3–*C*4	111.9	112.7	113.2
*N*3–*C*4	1.364	1.357	1.308	*N*3–*C*4–*C*5	127.6	129.2	129.8
*C*4–*C*5	1.392	1.391	1.438	*C*4–*C*5–*C*6	119.2	118.8	118.7
*C*5–*C*6	1.405	1.439	1.461	*C*5–*C*6–*N*1	111.9	109.3	110.1
*C*6–*N*1	1.398	1.440	1.441	*C*6–*N*1–*C*2	124.6	126.6	125.7
*C*4–*N*9	1.364	1.367	1.371	*N*3–*C*4–*N*9	126.2	125.9	128.0
*C*5–*N*7	1.405	1.381	1.333	*C*5–*C*4–*N*9	106.1	105.0	103.9
*N*7–*C*8	1.319	1.302	1.335	*C*4–*C*5–*N*7	109.6	110.9	110.6
*C*8–*N*9	1.369	1.384	1.367	*C*6–*C*5–*N*7	131.2	130.3	128.7
*C*2–*N*11	1.333	1.375	1.326	*C*5–*N*7–*C*8	104.2	104.7	105.1
*C*6–*O*10	1.239	1.209	1.195	*N*7–*C*8–*N*9	113.0	112.7	112.9
*N*1–*H*12		1.010	1.014	*C*8–*N*9–*C*4	107.0	106.7	106.8
*C*8–*H*13		1.078	1.079	*N*1–*C*2–*N*11	115.3	116.9	119.1
*N*9–*H*14		1.007	1.011	*N*3–*C*2–*N*11	120.0	119.6	115.4
*N*11–*H*15		1.008	1.008	*N*1–*C*6–*O*10	120.4	119.2	120.2
*N*11–*H*16		1.008	1.010	*C*5–*C*6–*O*10	127.7	131.5	128.8
				*N*1–*C*2–*N*11–*H*15		−33.1	0.0
				*N*3–*C*2–*N*11–*H*16		12.5	0.0

[a] Reference compound: guanine monohydrate [29].

Table 5
Calculated and experimental ionization potentials (in electron volts) of adenine, cytosine, guanine, and thymine

	MP2/631+G(*d*)[a]		B1LYP/6 311+G(*d*,*p*)[b]		Experimental	
	Vertical	Adiabatic	Vertical	Adiabatic	Vertical[c]	Adiabatic[d]
Adenine	8.58	8.18	8.16	7.95	8.44	8.26
Cytosine	8.82	8.74	8.62	8.47	8.94	8.68
Guanine	8.04	7.66	7.89	7.52	8.24	7.77
Thymine	10.33	8.85	8.90	8.66	9.14	8.87

[a] At the MP2/6-31G(*d*) geometry, from [33].
[b] At the B1LYP/6-311G(*d*,*p*) geometry, this work.
[c] From [31].
[d] From [32].

311+G(*d*,*p*)//B1LYP/6-311G(*d*,*p*) level are slightly underestimated with respect to the experimental values [31,32]. In particular, both the vertical and adiabatic IEs are too low by about 0.3 eV. The inclusion of the zero point vibrational energy (ZPVE) does not significantly affect the calculation of the adiabatic IEs since the ZPVE values for the neutral and radical cations are very similar. The previously published second order Møller Plesset (MP2) results show in general a slightly better agreement with the experiment even if the molecular geometry was kept planar during the MP2 geometry optimization [33]. However, it is important to underline that our DFT calculations are invariably affected by a spin contamination much lower than that issuing from UHF and UMP2 wave functions, thus allowing a safer investigation of spin-dependent properties [16,20].

3.2. Basic tools for the theoretical analysis of the molecular ion

Although it is clear that the energetics of fragmentation strongly depends on the relative stability of the daughter molecules and on the height of the energy barrier for the corresponding dissociation reactions, an analysis of the parent ions can nonetheless provide useful hints about the tendency to enter a given fragmentation channel.

First, it is important to establish which molecular orbital undergoes the largest changes in the ionization process. This is indeed the first step in an accurate study of the electronic structure of the ion and it is also relevant for the definition of the electronic rearrangements driven by the loss of one electron.

A second issue concerns the correctness of a localized picture of the molecular structure. We point out that, since the fragmentation process involves the breaking of well-defined chemical bonds, a "valence bond" description, complementary to the usual delocalized one, can often help the interpretation of the experimental results. Many different localization procedures have been proposed in the last decades, each one having its merits and its drawbacks. A critical comparison of the features of such localization techniques falls surely out of the scope of this article. We have resorted to the definition of NBOs [24]; this procedure relies on the determination of natural atomic orbitals, which transform every atomic subblock of the calculated density matrix in order to have occupancies close to 1 (bonding hybrids) or 2 (lone pairs) or 0 (Rydberg orbitals). After a suitable orthogonalization procedure, each bonding hybrid atomic orbital takes part in σ bonding and σ^* antibonding localized molecular orbitals with directly bound atoms. This method can thus decompose any given one-particle density matrix, possibly obtained by accurate ab initio computations, in terms of atomic orbitals participating in optimized electron–pair bonding functions, as in the Lewis structure picture.

The NRT [24c] is an extension of the NBO approach, which allows for the treatment of strongly delocalized systems. In short, this method determines which combination of Lewis "resonance structures" can best reproduce the exact NBO occupancies (q_i) of

the total wave function, through the minimization of the variational functional

$$d(w) = \min_{\{w\}} \left\{ \frac{1}{n} \sum_{i}^{n} (\tilde{q}_i - q_i)^2 \right\}^{1/2}$$

where $\tilde{q}_i$ is the localized resonance weighted occupancy, i.e. the occupancy corresponding to each resonance structure multiplied a weight factor w. Once the minimization procedure has determined the contribution of each resonance structure to the total wave function, the natural bond order (b_{AB}) between two atoms A, B can be simply calculated as

$$b_{AB} = \sum_{\alpha} w_\alpha b_{AB}^{\alpha}$$

where w_α is the weight and b_{AB}^{α} is the number of bonds connecting A and B in the α resonance structure. This method provides also an easy way to calculate the ionic and covalent contributions to the bond order.

The third important question to answer concerns the charge distribution in the ion. Standard ab initio packages can provide atomic charges according to different methods. The Bader's approach [34] is probably the most rigorous from a physical point of view (also for the definition of bond orders, vide infra), but it is very time consuming already for medium size molecules and can suffer from severe convergence difficulties. The atomic charges provided by the NPA [24b] represent a cheaper alternative, retaining the simplicity and the "chemical significance" of the MPA without their most serious drawbacks. They are intrinsically positive quantities, rather independent from the basis set being used, and allow also for a reliable treatment of ionic bonds.

Finally, GAPT atomic charges [23] also provide a basis set independent partition of the molecular charge and are particularly suited for the interpretation of spectroscopic observables like the IR intensities. They are indeed defined as the trace of the atomic polar tensor $\mathbf{V}^A$

$$V_{pq}^{A} = \partial \mu_p / \partial q_A, \qquad p, q = x, y, z$$

where μ_p are the Cartesian components of the molecular dipole moment and q_A are the Cartesian coordinates of the atom A. Since the derivative of the molecular dipole moment with respect to a given normal mode is proportional to the IR intensity for that mode, the difference in the GAPT charges of two directly linked atoms should be proportional to the intensity of the stretching mode for that bond, especially if it is not strongly coupled with other modes.

The key step in our study is to find out the bonds whose strength is largely reduced in the ionization process. The off-diagonal terms in the MPA provide a qualitative measure of the bond order between two atoms, which in turn is related to the strength of the bond. NRT is able, instead, to directly provide bond orders (vide supra) in accordance to the simple Lewis picture of the molecules.

As a final point, the comparison between the ground state geometry of the molecular ion and that of the neutral parent is relevant in all the above analysis.

In the following the ionization process of thymine is analyzed in detail and it is compared to that of cytosine. In addition, we will also report some concise considerations on the purine bases (adenine and guanine).

3.3. Radical cations of the DNA bases and their fragmentation

3.3.1. Thymine

In Table 1 are reported the optimized structures of thymine and of its radical cation. Upon ionization the C5–C6, C6–N1, and N1–C2 bonds undergo the largest modifications. In particular, the C5–C6 bond length increases by 0.06 Å (from 1.347 to 1.407 Å), while the N1–C6 bond is shortened from 1.379 to 1.322 Å. The N1–C2 bond also increases from 1.388 to 1.451 Å. The changes in the other bond lengths are less significant. The lengths of both the C–O bonds and of the C2–N3 bond are slightly reduced. Also the bond between C5 and the methyl group (C9) is shortened by about 0.03 Å. The N–H bond lengths are all around 1.01 Å while the C–H bonds lie between 1.08 Å (on the C5–C6 double bond) and 1.09 Å (in the methyl group). As expected, the bonds involving

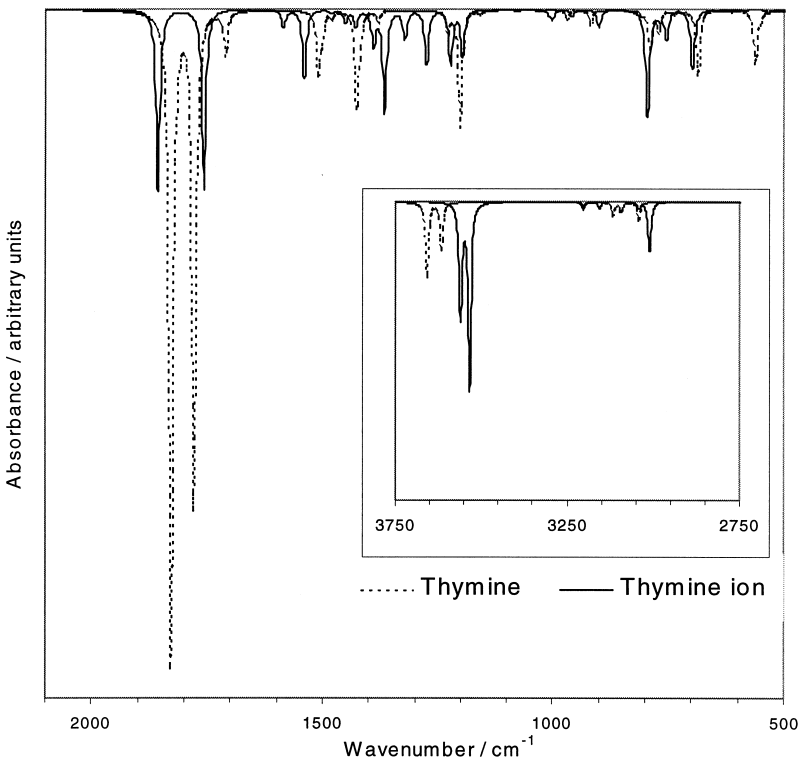

Fig. 2. Simulation of the IR absorption spectra of neutral thymine and its radical cation. The ab initio vibrational normal modes have been computed at the B1LYP/6-311G(*d*,*p*) level of theory.

hydrogen atoms are only indirectly affected by the ionization since the electron is removed from a π molecular orbital. Due to the rigid ring structure, the changes in the bond angles are generally negligible. The methyl group does not modify its orientation in the charged system.

Fig. 2 shows the simulation of IR absorption spectra of thymine and its radical cation, on the basis of the vibrational normal mode analysis carried out at the B1LYP/6-311G(*d*,*p*) level of theory. As a matter of fact, the ability of predicting spectroscopic observables for transient species like molecular radical cations, is very attractive in itself, since those results cannot be easily obtained experimentally. Moreover, the features of the IR spectra and the underlying vibrational normal modes, are strongly related to the geometric and electronic structure of the system. In particular, dealing with ionization processes, the changes in the relative strength of the various bonds affect the frequencies of the IR absorption peaks and the charge re-distribution can be enlightened by the observed (or predicted) intensities.

A detailed comparison between the calculated IR spectra of the neutral and charged forms of thymine is not easy since the in general the normal modes are not simply shifted in frequency, but also recombined to a large extent. However, a few interesting features of Fig. 2 can be highlighted.

First of all, the two C=O stretching modes are not coupled with any ring mode and their frequencies are thus simply shifted by about 20–30 cm^{-1}. The C2O7 peak is shifted from 1829 to 1857 cm^{-1} in accordance with its strengthening predicted by our analysis of the electronic structure rearrangement (see the following). On the contrary, the frequency of the C4O8 stretching decreases from 1780 to 1757 cm^{-1}. The substantial difference in the intensity of the C=O stretching absorptions can be effectively explained in

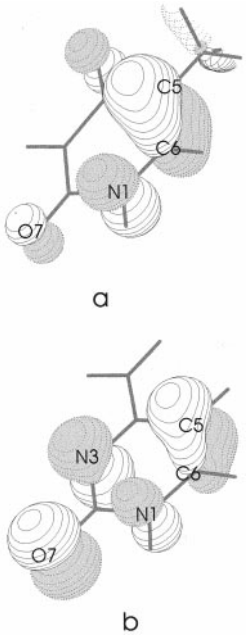

Fig. 3. Single occupied molecular orbital (SOMO) of (a) thymine and (b) cytosine radical cations obtained by B1LYP/6-311G(*d*,*p*) calculations.

terms of the decrease of the bond dipole computed by GAPT atomic charges. In the neutral thymine these latter are: C2 +1.27, O7 −0.87, C4 +1.08, and O8 −0.80 a.u., whereas in the radical cation the values are as follows: C2 +1.04, O7 −0.56, C4 +0.76, and O8 −0.51 a.u. A second noteworthy feature concerns the coupled C5=C6 and C6–N1 stretching band, which appears at 1712 cm^{-1} in the spectrum of the neutral molecule, and is significantly shifted to 1586 cm^{-1} in the charged species, with increased contribution from N1=C6 stretching.

The comparison between the molecular orbitals in neutral and in charged thymine, suggests that the electron is ejected by a bonding π orbital [see Fig. 3(a)] involving mainly atoms belonging to the pyrimidine ring. On the other hand the corresponding orbitals of the other bases have significant contributions from the exocyclic atoms [see, e.g. the singly occupied molecular orbital (SOMO) of cytosine in Fig. 3(b)]. As a likely consequence the mass spectrum of thymine exhibits the greatest tendency toward fragmentation of the ring. When the electron impact energy is 70 eV, the peak corresponding to the molecular ion is just the third in relative intensity, whereas for cytosine (see the following) the molecular ion peak is always the most intense one, also at high ionization energy.

Even if there are small contributions from N1, O7, and O8, the ionized molecular orbital corresponds essentially to the C5–C6 π bond, (with a larger contribution of C5). This explains the weakening of the C5–C6 bond predicted by the above vibrational analysis and the decrease in the atomic population of the oxygen atoms, which leads, in turn, to a decreased intensity of the C=O stretching modes.

The ionization process should thus induce both partial positive charges and significant spin populations on C5 and C6. The NPA shows indeed that C5 exhibits the largest change in electron population upon ionization (+0.26 a.u.). Moreover, the methyl group (C9) becomes more positive by 0.17 a.u. and this is consistent with the increase in the positive charge on C5. The largest atomic spin density obtained by the MPA (0.54 a.u.) is localized on C5. On the other hand, the increase in positive charge and spin density on C6 is remarkably lower: its contribution to the SOMO is smaller than that of C5. Furthermore, the contribution from N1 suggests that the partial positive charge on C6 can be delocalized on the adjacent nitrogen atom through the formation of a partial double N1–C6 bond (see the resonance structure depicted in Fig. 4). This is also consistent with the fact that the electron is removed from a molecular orbital in which a nodal surface is located between N1 and C6 (antibonding) thus increasing the bond order. This picture is further confirmed by the MPA, which shows how the ionization process leads to a decrease of about 30% in the Mulliken overlap population (MOP) between C5 and C6 and to an increase of about 15% in the N1–C6 MOP. It is important to underline that these results still hold (even if with lower relative variation) when the calculation of the ionic species is performed at the geometry of the neutral parent, showing that these features are strongly related to the electronic structure of thymine. Since the N1 atom acquires a formal partial positive charge, it can no longer take part in the amidic partial

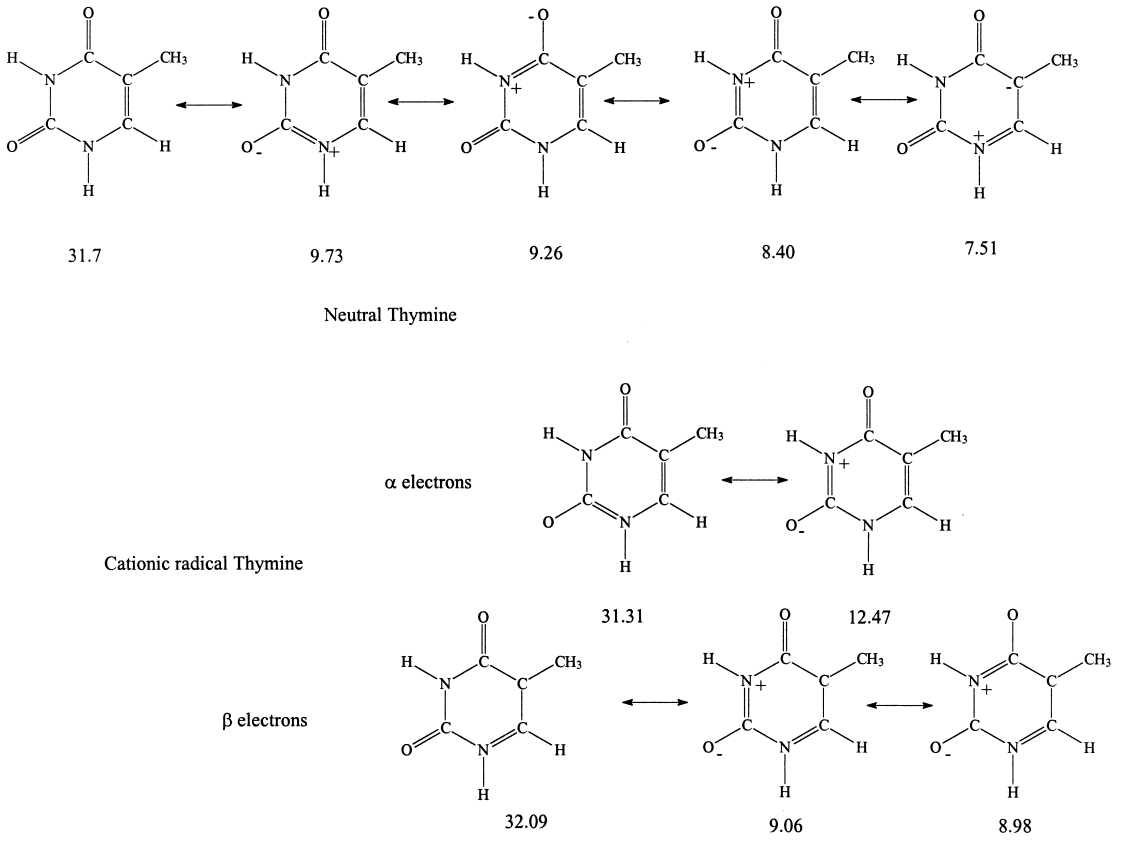

Fig. 4. Most important resonance structures (relative weight > 7.5%) as predicted by the natural resonance theory analysis for the neutral and the radical cationic thymine.

double bond with the C2–O7 carbonyl (see also the discussion on NRT in the following). Thus, the reduction of the C2–N1 bond order (and the strengthening of the C2=O7, as witnessed by the above vibrational spectra) can be anticipated and indeed the MOP decreases by about 20%.

The strengthening of the N1–C6 bond is expected to have consequences also on the other side of the molecule. Since the N^+=C–O^- resonance structure is now possible for the C2–N3 bond only, the bond order is increased (the MOP increases by about 10%). All these results find a nice correspondence in the NRT (see Fig. 4). The N1–C6 bond order increases indeed from 1.07 up to 1.51, with a decrease of the C5–C6 and N1–C2 ones from 1.82 and 1.06 to 1.42 and 0.98, respectively. For what concerns the relative weight of the resonance structures, for the α electrons the NRT provides a description corresponding to the Lewis structure of the neutral thymine, but for the β electrons it predicts a double N1–C6 bond, a single C5–C6 bond and a "lone pair" electron on C5. Moreover, the weight of resonance structures with a single C2–O7 bond and a double C2=N3 bond is about the double of those involving a single C2–O7 and a double C2=N1 bond, whereas in the neutral form their relative weight is almost the same. Interestingly the cation (mostly for β electrons) is characterized by a remarkably increased weight of resonance structures involving the breaking of N1–C2 and N3–C4 bonds.

In summary, the picture emerging from the analysis of the DFT results is that of an incipient breaking

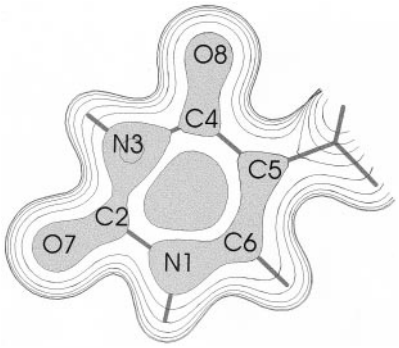

Fig. 5. π electronic density of the thymine ion obtained by B1LYP/6-311G(d,p) calculations.

of the N1–C2 bond, with a simultaneous formation of a double N1=C6 bond and a single C5–C6 bond. This picture is clearly visualized in Fig. 5, which shows the total π electronic density of the thymine ion: N1–C2 and N3–C4 are single bonds, with vanishing contributions by the π electrons, whereas the N1–C6 bond has a significant π contribution.

All these results are fully consistent with the mass spectrum of thymine. As a matter of fact the most important feature in the fragmentation pattern of thymine is the loss of the HNCO group through a "so-called" retro Diels-Alder (RDA) reaction [35,36]. This is a well-known reaction in which "cyclohexene like" molecules break up into a two atom fragment with one double bond ("ethylene like") and a four atom moiety with two double bonds ("butadiene like"). As a further step towards the theoretical study of the fragmentation path we have studied in some detail this reaction: first, we have characterized thermodynamically the possible products of the expulsion of an HNCO fragment from the thymine. As a matter of fact, even if our analysis of the molecular ion suggests the breaking of the N1–C2 and N3–C4 bonds with the dissociation of the O7=C2–N3–H11 fragment (P1 path), two other fragmentations are in principle possible, involving the breaking of N1–C6 and C2–N3 (P2 path) or C2–N3 and C4–C5 (P3 path) bonds, respectively (see Fig. 6).

We have optimized, at the B1LYP/6-311G(d,p) level of theory, the geometry of the cationic fragments deriving from the three possible dissociation paths:

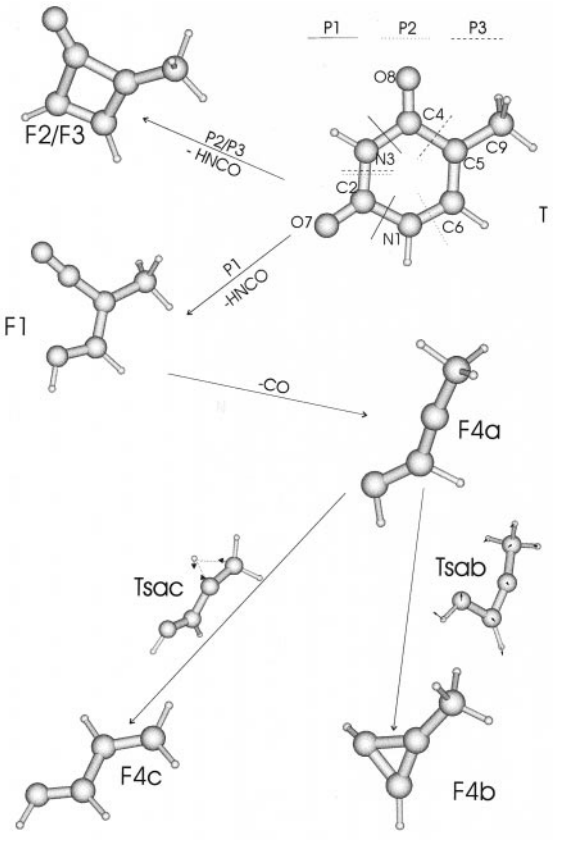

Fig. 6. Most relevant stationary points involved in the ejection of the HNCO moiety from the thymine ion and in the subsequent loss of the CO group. TSac is the saddle point for the 1,2 hydrogen shift yielding F4c from F4a (one imaginary frequency at 830i cm^{-1}). TSab is the saddle point for the ring closure yielding F4b from F4a (one imaginary frequency at 137i cm^{-1}).

the minimum energy structures are collected in Fig. 6. Only fragment F1 (the one deriving from P1 dissociation) exhibits a stable minimum in the open form, whereas both F2 and F3 (deriving from P2 and P3) are predicted to cyclize in the same four membered ring. Thus only F1 is structurally similar to the product of a RDA reaction, which should involve a dienophile and a diene in open form. Moreover F1 is more stable than F2/F3, by 1.3 kcal/mol.

From the kinetic point of view, as a first step toward a complete characterization of the fragmentation path, we have analyzed in detail the P1 pathway, which should be the most likely. A closer inspection of Fig. 5 shows that the P2 and P3 paths would

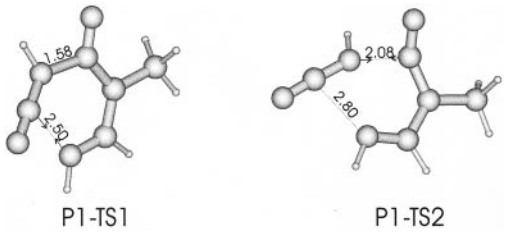

Fig. 7. Saddle points for the ejection of the HNCO moiety from F1.P1–TS1 is the first saddle point in the P1 reaction path; one imaginary frequency at $108i$ cm^{-1} P1–TS2 is the second saddle point in the P1 reaction path; one imaginary frequency at $130i$ cm^{-1}.

involve the breaking of two and one partial double bonds, respectively, whereas all the bonds broken in the P1 paths have negligible double bond character. We have then located at the B1LYP/6-311G(d,p) level the saddle points for the dissociation of the C2–O7–N3–H moiety from the thymine ion. It is indeed interesting to verify if the first fragmentation reaction can be interpreted as a traditional "RDA" reaction. Our calculations predict a stepwise fragmentation characterized by two saddle points. The first saddle point (P1–TS1 in Fig. 7) corresponds to the cleavage of the N1–C2 bond (N1–C2 distance about 2.5 Å) with the simultaneous weakening of N3–C4 bond, whose bond length increases up to 1.58 Å: this saddle point is about 42 kcal/mol less stable than the molecular ion. After the formation of a very unstable intermediate, in the second step (P1–TS2 in Fig. 7) the breaking of the N3–C4 bond is accomplished (see Fig. 7); P1–TS2 lies about 46 kcal/mol above the thymine ion. After P1–TS2 a scan of the potential energy surface reveals the existence of a flat region about 6–7 kcal/mol below the separated fragments, corresponding to the formation of an adduct between a cationic moiety (F1) and an highly unsaturated molecule (HNCO). However this shallow minimum should not be relevant to the fragmentation process, because the two fragments have a quite high kinetic energy available for the separation.

Since the reliability of DFT models for conventional Diels-Alder reactions has been unquestionably proven [37], our results raise some doubts against the classification of this fragmentation as RDA. As a matter of fact, the conventional Diels-Alder reactions follow a concerted mechanism [37,38], and also the RDA fragmentation of 4-vinylcyclohexene has been predicted to be concerted [35].

The analysis of the frontier orbitals of the HNCO moiety shows that the π electronic density at the carbon atom is low as the latter lies on a nodal surface in the highest occupied molecular orbital (HOMO) of the three centers, four electrons π system. This could explain why in the first saddle point, C2 is found outside the ring plane whereas N3 is coplanar with the C4–C5–C6–N1 moiety. Such a structure does not resemble the saddle point expected for a Diels Alder reaction where the dienophile lies parallel to the diene plane. Finally, it is worth noting that the first bond being broken is C2–N1, i.e. the one we predicted to be the weakest on the basis of our analysis of the thymine ion. In spite of the above remarks, in the following, for the sake of concision, we design as RDA all the reaction involving the expulsion of a HNCO and of a NCO fragment.

After the expulsion of HNCO, the resulting fragment F1 is expected to loose quite easily a carbonyl group, yielding the second important peak of the low energy mass spectrum [14].

We also studied the product F4 in order to find out the relative stability of the isomers structurally more similar to the parent compound. We located three stable minima, F5a, F5b and F5c in Fig. 6. F5a is the compound resulting just from the expulsion of CO from F4, F5b is its cyclic analogue, whereas F5c derives from an 1,2 hydrogen shift between C9 and C5. As previously shown [39], F5c is the most stable isomer at the B1LYP/6-311G(d,p) level (about 14.0 kcal/mol more stable than F5b and 38.2 kcal/mol more than F5a). In the hypothesis that the expulsion of CO occurs without significant rearrangements of F4, thus producing the fragment F5a, we have located the saddle points for the 1,2 hydrogen shift, which yields F5c, and for the ring closure, which yields F5b. The barrier of the former reaction is 6.8 kcal/mol (saddle point TSac in Fig. 6), whereas the barrier height for the ring closure is just 1 kcal/mol (saddle point TSab in Fig. 6). Thus, although F5a is the thermodynamically favored compound, F5b should be

kinetically more accessible. Moreover, it is worth noting that the fragmentation path of uracil is rather similar to that of thymine (RDA reaction followed by the expulsion of CO) [14], even if uracil lacks the methyl group on C5 and, as a consequences, a F5c-like intermediate. F5b is more stable than F5a, showing that the cyclization reaction does not require the expulsion of an hydrogen atom, as previously suggested [14]. However, without a further analysis of the potential energy surfaces, it is not possible to determine whether the expulsion of CO from F1 (which is predicted to be endothermic by at least 38.4 kcal/mol) occurs in a concerted step with the 1,2 hydrogen shift, in a concerted step with the ring closure or, conversely, it gives first the open chain fragment F5a which subsequently yields F5c (see Fig. 6).

The analysis of the electronic structure of thymine radical cation gives also some insights on the reason why its mass spectrum does not exhibit any peak due to the loss of a methyl group, whereas this peak is present in the spectrum of 6-methyl uracil [14]. We have indeed pointed out that the largest fraction of the positive charge is localized on C5 and this makes more difficult the cleavage of the bond with the electron-donating methyl group. The presence of the methyl is far less important when it is bound to C6, where it can only help the partial delocalization of the positive charge on N1.

3.3.2. Cytosine

Let us now examine cytosine, the other pirimydinic DNA base. The optimized geometric parameters of neutral and cationic species are listed in Table 2. Many bonds are affected by the ionization. The C2–O7, N3–C4 and C5–C6 bond lengths increase in the ion with respect to the neutral system by about 0.025–0.030 Å, whereas C2–C3, C4–N8, and N1–C6 bonds are shorter by almost the same amount. Smaller changes are observed for the N1–C2 and C4–C5 bonds. As in the case of thymine, the lengths of H–C and H–N bonds are only slightly modified. The ring structure prevents also large changes in the bond angles. Noteworthy, the exocyclic amino group shows a slight pyramidalization in the neutral molecule, which is completely lost in the ion.

In this compound the electron is ejected from a molecular orbital rather similar to that of thymine [see Fig. 3(b)], but with a remarkably larger contribution from the p_z orbitals of O7 and N3. Due to the different topology of the π system, this orbital can be considered the result of the interaction between a "butadiene like" HOMO (N3=C4–C5=C6), and the C=O π bond.

This result has a great influence on the charge distribution in the molecular ion. Indeed, the atom that acquires the largest fraction of the positive charge is the oxygen O7 (its NBO population goes from −0.61 a.u. to −0.30 a.u.) which also carries the highest spin density (0.54 a.u. to be compared with 0.34 a.u. on C5). The localization of the electronic density depletion mostly on an exocyclic atom could be related to the resistance of cytosine against fragmentation, as shown by the high relative intensity of the molecular ion peak. The most remarkable changes in the MOP upon ionization include the decrease of the N3–C4 overlap population and the increase of the C4–N8 one. Indeed, the loss of an electron weakens the N3–C4 double bond and favors the formation of a partial double bond between C4 and the amino substituent.

As a matter of fact, the NPA predicts a single N3–C4 and a double C4–N8 bond for both α and β electrons. As for thymine, the β electron density is consistent with a single C5–C6 bond.

The electronic structure just described can be expected to undergo a RDA reaction, as in the case of thymine. Since this reaction, as seen above, is favored by the formation of the C4–N8 double bond, it is likely to be easier if the nitrogen looses a hydrogen atom. This hypothesis is confirmed by the experimental mass spectra, in which the peak due to expulsion a NCO radical (one of the products of the RDA reaction) has almost the same intensity as the one due to the simultaneous loss of the NCO radical and a H radical (possibly as a single HNCO species).

The presence of a more electronwithdrawing oxygen atom can account for the other important feature of the low energy mass spectra of cytosine, which is absent in the mass spectra of thymine, i.e. the loss of

the carbonyl group from the molecular ion [14]. Indeed, the carbonyl group can act as an electron sink for the σ bonds of the carbon. Moreover, the resulting $C_3H_4N_3^+$ species (in cyclic or open form) is also expected to be rather stable, being able to effectively delocalize the positive charge. The loss of a neutral CO molecule is a rather common feature in the fragmentation patterns of compounds with a carbonyl group bonded to an aromatic cycle [40].

3.3.3. Guanine and adenine

The optimized structures of the neutral and charged forms of the pyrimidinic bases are collected in Tables 3 and 4. Indeed, adenine and guanine undergo very similar structural modifications. In both compounds, the C2–N3–C4–C5–N7–C8 bond sequence is the most affected, showing significant changes in the bond lengths. These changes are all around 0.04–0.05 Å in absolute value, but with alternating directions. The C2–N3, C4–C5, and N7–C8 bonds are shortened while the N3–C4 and C5–N7 ones are lengthened. The remaining bonds in the pyrimidine rings are modified to smaller extents ($\leq$0.03 Å).

The geometry of the exocyclic amino group in guanine is also noteworthy. In the neutral compound it is slightly pyramidalized whereas in the cation it becomes planar. The NH_2 group is in the right position to enter the conjugation of the C2–N3–C4–C5–N7–C8 bond sequence, but this happens only in the charged compound where the C2–N11 bond length is shortened by 0.05 Å. This is consistent with the involvement of the nitrogen lone pair in the conjugation and with the subsequent planarization of the amino group. The presence of a pyrimidine ring in guanine and adenine makes their fragmentation patterns quite similar to those of cytosine and thymine. In guanine the electron is removed from the ex-atriene-like HOMO C2=N3–C4=C5–N7=C8 [see Fig. 8(a)] which has some contribution also from the amino lone pair, thus suggesting a rearrangement to an electronic structure with increased N3–C4 and C5–N7 bond orders.

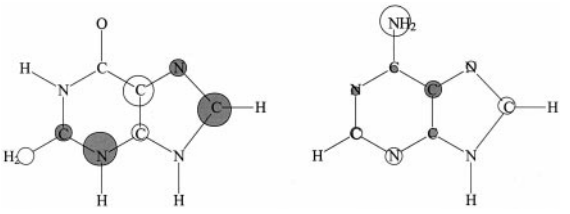

Fig. 8. Schematic drawing of the SOMO of (a) guanine and (b) adenine radical cations.

Indeed, the NPA predicts for β electrons a double bond character for the N1–C2 and C2–N11 bonds, and only a single bond between C2 and N3. These results suggest the possibility of a RDA reaction in which a stable cyanamide group (N1–C2–N11) is ejected. This is actually the most important feature in the fragmentation pattern of the guanine molecular ion. The formation of the cyanamide group is also supported by the increased double bond character of C2–N11, suggested by shorter bond length and 16% increase in the MOP.

For adenine, the main fragmentation path involves the loss of three HCN units and from the high-energy mass spectrum (70 eV) it is not possible to establish which is the actual sequence of losses, i.e. in which order the HCN (or HNC) units dissociate from the molecular ion [15].

The KS molecular orbitals are similar to those of guanine and their analysis shows that the ionization process leads to the formation of a C6–N10 double bond, while the aromatic structure of the pyrimidine ring has a tendency toward the formation of N1–C2 and N3–C4 double bonds. This suggests that the N1C2H group is the best leaving group as also supported by the strong decrease of the N1–C2 bond length with the simultaneous increase of the C2–N3 and N1–C6 ones. However, without a thorough kinetic analysis this can be just a tentative proposal. The analysis of the MOP shows that other HCN fragments could be ejected as well (e.g. HC8N7, which can leave the aromatic ring unchanged). A definitive assessment of the loss sequence would require a far more detailed analysis of the energetics of the available fragmentation paths.

4. Conclusions

In this article we have presented a detailed DFT study of the DNA bases and of their cationic radicals. The comparison between the electronic structures of the cationic species and those of the neutral parent compounds provides useful insights about the main features of the fragmentation patterns recorded in the mass spectra. Our calculations show that the electronic and geometric rearrangements caused by the ionization process are consistent with the experimental evidence that the removal of HNCO or NCO moieties represents the main dissociation pathway for all the DNA bases. We have then analyzed in some detail the fragmentation path of thymine, showing that a stepwise process is the most likely for the expulsion of the HNCO moiety. This results, together with an analysis of the frontier orbitals of the resulting fragments, make questionable the classification of this reaction as RDA. It is interesting to underline that there is a nice matching between the results of the kinetic characterization of the thymine fragmentation and those of the analysis of the electronic structure of the thymine ion. For example, the N1–C2 bond is broken in the first step of the fragmentation reaction, in agreement with our conclusion that N1–C2 is the weakest bond of the thymine ring. Furthermore, the analysis of DFT results allows to explain some peculiar features of the mass spectra of thymine and cytosine; i.e. the absence of peaks due to the ejection of a methyl radical in the former and the remarkable height of the peak due to the loss of CO in the latter.

These results support our opinion that a careful study of the molecular ion can be useful to ascertain which bonds are more weakened by the ionization process, giving valuable information on the most likely dissociation paths. Of course the analysis of the electronic and geometric structure of the molecular ion *alone* can just give some "propensity rules" for the fragmentation pathway, whereas a full rationalization of the experimental mass spectra would require a complete thermodynamic and kinetic characterization of all the possible dissociation paths.

Our study underlines also the usefulness of "traditional" theoretical analyses like those based on bond orders and atomic charges in accordance with the chemical picture of molecules as formed by well defined building blocks: localized σ bonds, lone pairs and π bonds (whose degree of delocalization is measured by the relative importance of the possible resonance structures). At the same time, the reliability of this approach increases if the equilibrium geometry and the corresponding electron density are calculated by means of sophisticated ab initio techniques including the effects of electron correlation. From this point of view, DFT calculations provide very accurate equilibrium geometries also for open-shell systems, with negligible spin contamination. In our case the reliability of the B1LYP calculations is confirmed by the agreement between experimental and calculated geometries and ionization energies.

Finally, this work allowed us to describe some effective theoretical tools for the analysis of a standard ab initio output in order to rationalize and, if possible, predict the main fragmentation pathways in the experimental mass spectra. In our opinion this could be very useful for experimentally oriented chemists, since high level computations and the subsequent theoretical analysis of the results, can be nowadays performed quite easily by standard ab initio packages.

References

[1] F.W. Mc Lafferty, Interpretation of Mass Spectra, Benjamin, New York, 1966.
[2] M.C. Hamming, N.G. Foster, Interpretation of Mass Spectra of Organic Compounds, Academic, New York, 1972.
[3] (a) H.M. Rosenstock, M.B. Wallenstein, A.L. Warhaftig, H. Eyering, Proc. Natl. Acad. Sci. USA 38 (1952) 667; (b) H.M. Rosenstock, M. Krauss, in Mass Spectroscopy of Organic Ions, F.W. Mc Lafferty (Ed.), Academic, New York, 1964, pp. 1–64.
[4] J.C. Lorquet, Mass Spectrosc. Rev. 7 (1982) 63.
[5] Born and Oppenheimer, Ann. Phys. 84 (1927) 457.
[6] (a)J.C. Lorquet, Gazz. Chim. Ital. 108 (1978) 145; (b) J.C. Lorquet, D. Dehareng, C. Sannen, G. Raseev, in Quantum Theory of Chemical Reactions, R. Daudel (Ed.), Reidel, Dordrecht, 1980, p. 241.
[7] M.J.S. Dewar, R.C. Dougherty, The PMO Theory of Organic Chemistry, Plenum, New York, 1975; P.V. Schleyer, in Advances in Mass Spectroscopy, J.F.J. Todd (Ed.), Wiley, New York, (1985), p. 287; H. Schwarz, ibid. p. 13.

[8] More than 30 papers dealing with ab initio computations has been appeared in Int. J. Mass. Spectrom. since 1997.
[9] (a) A.G. Baboul, L.A. Curtiss, P.C. Redfern, K. Raghavachari, J. Chem. Phys. 110 (1999) 7650; (b) G.A. Petersson, D.H. Malick, W.G. Wilson, J.W. Ochtorski, J.A. Montgomery Jr., M.J. Frisch, ibid. 109 (1998) 10570.
[10] J.A. Pople, R. Krishnan, H.B. Schlegel, J.S. Binkley, Int. J. Quantum Chem. XIV (1978) 545.
[11] (a) R.G. Parr, W. Yang, Density Functional Theory of Atoms and Molecules, Oxford University Press, New York, 1988; (b) Recent Advances in Density Functional Methods, D.P. Chong (Ed.), World Scientific, Singapore, 1995, p. 287.
[12] (a) M.J. Bearpark, M.A. Robb, H.B. Schlegel, Chem. Phys. Lett. 223 (1994) 269; (b) F. Bernardi, M.A. Robb, M. Olivucci, Chem. Soc. Rev. 25 (1996) 321.
[13] J.B. Foresman, A.E. Frisch, Exploring Chemistry with Electronic Structure Methods, 2nd ed, Gaussian Inc., Pittsburgh, PA, 1996.
[14] J.M. Rice, G.O. Dudek, M. Barber, J. Am. Chem. Soc. 87 (1965) 4569.
[15] J.M. Rice, G.O. Dudek, J. Am. Chem. Soc. 89 (1967) 2719.
[16] F. Jolibois, J. Cadet, A. Grand, R. Subra, V. Barone, N. Rega, J. Am. Chem. Soc. 120 (1998) 1864.
[17] S.D. Wetmore, R.J. Boyd, L.A. Eriksson, J. Phys. Chem. 102 (1998) 5369, 7484, 9332, 10602, and references therein.
[18] C. Adamo, V. Barone, Chem. Phys. Lett. 274 (1997) 242.
[19] A description of basis sets and standard computational methods can be found in [13].
[20] V. Barone, in Recent Advances in Density Functional Methods, D.P. Chong (Ed.), World Scientific, Singapore, 1995, p. 287.
[21] GAUSSIAN 98, M.J. Frisch, G.W. Trucks, H.B. Schlegel, G.E. Scuseria, M.A. Robb, J.R. Cheeseman, V.G. Zakrzewski, J.A. Montgomery Jr., R.E. Stratmann, J.C. Burant, S. Dapprich, J.M. Millam, A.D. Daniels, K.N. Kudin, M.C. Strain, O. Farkas, J. Tomasi, V. Barone, M. Cossi, R. Cammi, B. Mennucci, C. Pomelli, C. Adamo, S. Clifford, J. Ochterski, G.A. Petersson, P.Y. Ayala, Q. Cui, K. Morokuma, D.K. Malick, A.D. Rabuck, K. Raghavachari, J.B. Foresman, J.V. Ortiz, A.G. Baboul, J. Cioslowski, B.B. Stefanov, G. Liu, A. Liashenko, P. Piskorz, I. Komaromi, R. Gomperts, R.L. Martin, D.J. Fox, T. Keith, M.A. Al-Laham, C.Y. Peng, A. Nanayakkara, M. Challacombe, P.M.W. Gill, B. Johnson, W. Chen, M.W. Wong, J.L. Andres, C. Gonzalez, M. Head-Gordon, E.S. Replogle, J.A. Pople, Gaussian, Inc., Pittsburgh, PA, 1998.
[22] R.S. Mulliken, J. Chem. Phys. 23 (1955) 1833.
[23] J. Cioslowski, J. Am. Chem. Soc. 111 (1989) 8333.
[24] (a) J.P. Foster, F. Weinhold, J. Am. Chem. Soc. 102 (1980) 7211; (b) A.E. Reed, F. Weinhold, J. Chem. Phys. 78 (1983) 4066; (c) E.D. Glendening, F. Weinhold, J. Comp. Chem. 19 (1998) 593.
[25] E.D. Gluendening, J.K. Badenkoop, A.E. Reed, J.E. Carpenter, F. Weinhold, Theoretical Chemistry Institute, University of Wisconsin Press, Madison, WI, 1996, NBO 4.0.
[26] R. Gerdil, Acta Cryst. 14 (1961) 333.
[27] D.L. Barker, R.E. Marsh, Acta Cryst. 17 (1964) 1581.
[28] R.F. Stewart, L.H. Jensen, J. Chem. Phys. 40 (1964) 2071.
[29] U. Thewalt, C.E. Bugg, R.E. Marsh, Acta Cryst. B 27 (1971) 2358.
[30] J. Leszczynski, Int. J. Quantum. Chem.: Symp. 19 (1992) 43, and references therein.
[31] N.S. Hush, A.S. Cheung, Chem. Phys. Lett. 34 (1975) 11.
[32] V.M. Orlov, A.N. Smirnov, Y.M. Varshavsky, Tetrahedron Lett. 48 (1978) 4377.
[33] M.D. Sevilla, B. Besler, A.-O. Colson, J. Phys. Chem. 99 (1995) 1060.
[34] R.F.W. Bader, Atoms in Molecules: A Quantum Theory, Oxford University Press, Oxford, 1990.
[35] R.C. Dougherty, J. Am. Chem. Soc. 90 (1968) 5780, 5788.
[36] (a) H. Budzikiewicz, J.I. Brauman, C. Djerassi, Tetrahedron 21 (1965) 1855; (b) R.W. Reiser, Org. Mass. Spectrom. 2 (1969) 467; P.M. Draper, D.B. MacLean, Can. J. Chem. 46 (1968) 1499.
[37] V. Barone, R. Arnaud, Chem. Phys. Lett. 251 (1996) 393; V. Barone, R. Arnaud, P.Y. Chavant, Y. Vallee, J. Org. Chem. 61 (1996) 5121; V. Barone, R. Arnaud, J. Chem. Phys. 106 (1997) 8727.
[38] K.N. Howk, J. Gonzales, Y. Li, Acc. Chem. Res. 28 (1995) 81.
[39] S.G. Lias, J.E. Bartmess, J.F. Liebman, J.L. Holmes, R.D. Levin, W.G. Mallard, J. Phys. Chem. Ref. Data 17 (1988) suppl. 1.
[40] (a) J.H. Beynon, A.E. Williams, Appl. Spectrosc. 13 (1960) 101; (b) J.H. Beynon, R.A. Saunders, A.E. Williams, The Mass Spectra of Organic Molecules, Elsevier, New York, 1968, pp. 205–210.